Available online at www.sciencedirect.com

SCIENCE DIRECT

Experimental Neurology 196 (2005) 138 – 152

Experimental Neurology

www.elsevier.com/locate/yexnr

Coding of peripheral electrical stimulation frequency in thalamocortical pathways

He Yang[a], Jing-Yu Chang[b], Donald J. Woodward[b], Luiz A. Baccalá[c], Ji-Sheng Han[a], Fei Luo[a,*]

[a]Neuroscience Research Institute and Department of Neurobiology, Peking University, 38 Xue-Yuan Road, Beijing 100083, P.R. China
[b]Department of Physiology and Pharmacology, Wake Forest University Health Science, Winston-Salem, NC 27157, USA
[c]Telecommunications and Control Engineering, Escola Politecnica, University of Sao Paulo, Brazil

Received 18 December 2004; revised 4 July 2005; accepted 20 July 2005
Available online 29 August 2005

Abstract

Frequency information of the environment is an important feature for sensory perception. It has been demonstrated that cortical and thalamic neurons exhibited frequency-specific responses to peripheral stimulation. In the present study, we investigated the effects of 1–100 Hz peripheral electrical stimulations on various thalamic and cortical areas in awake rats. We used chronically implanted microelectrode arrays to record neural activities from the anterior cingulate cortex, primary somatosensory cortex, and medial dorsal and ventral posterior thalamus. The results revealed that cortical and thalamic neurons exhibited frequency-specific responses at both single-neuron and ensemble levels. Clusters of neurons responded to different frequency ranges with changes of both the peak firing rates and the phases of the peak responses in a stimulation cycle. Partial directed coherence analysis showed that information flowing between these recorded areas is also enhanced or inhibited in some frequency-specific pattern during stimulation. These evidences suggest that central nervous system may code environmental frequency information mainly with the activation of selected neural circuits according to their own intrinsic electrical properties. These properties, in turn, may facilitate or inhibit their responses when stimulation with specific frequency information arrives.

Keywords: Frequency perception; Frequency-specific response; Anterior cingulate cortex; Primary somatosensory cortex; Thalamus; Partial directed coherence; Transcutaneous electric nerve stimulation; Analgesia

Introduction

Perception of frequency information in the environment is an important function of the sensory system. As two examples, visual and auditory systems specifically develop to distinguish frequencies of electromagnetic waves and sound waves, respectively. Recent studies have revealed that peripheral somatosensory stimulation in certain frequency ranges can induce specific neural responses in the cortex and thalamus. By stimulating vibrissae at frequencies from 1 to 40 Hz, Garabedian et al. (2003) observed that neurons in primary somatosensory cortex (SI) exhibited the highest total spiking rate to repetitive stimuli between 5 and 10 Hz. Such frequency-dependent processing was found throughout the vibrissa sensory system. For instance, ventral posterior thalamus (VP) and SI neurons showed a wide variety of frequency-dependent filter characteristics, including 'low pass', 'high pass', and 'band-pass' (Ahissar et al., 2000; Fanselow and Nicolelis, 1999; Moore, 2004). These evidences suggest that thalamocortical pathways may have the ability to code frequency information in this range of stimuli.

Studies on the effect of peripheral electrical stimulation revealed that specific frequencies applied to certain body sites may have specific effect on the central nervous system. For example, peripheral stimulation of 2 Hz produces a significant increase in the release of enkephalin, whereas 100 Hz increases the release of dynorphin in the spinal cord level (Fei et al., 1986; Han and Sun, 1990; Han, 2003; Ulett et al., 1998). Also, it has been clinically demonstrated that only high-frequency deep brain stimulation is effective in the treatment of Parkinson's disease and other movement

* Corresponding author. Fax: +86 10 82801010.
E-mail address: fluo@bjmu.edu.cn (F. Luo).

0014-4886/$ - see front matter © 2005 Elsevier Inc. All rights reserved.
doi:10.1016/j.expneurol.2005.07.019

disorders (Lozano, 2001; Tarsy, 2001). Recent development of the Brain-Computer Interconnection (BCI) technique also showed that there exists frequency-dependent neural response to flicker stimulations (Gao et al., 2003; Kalcher et al., 1996; Pfurtscheller et al., 1995–96, 2000; Pregenzer and Pfurtscheller, 1999). In short, the effects of peripheral stimulation were often frequency-specific. These evidences also suggest that the central nervous system must have specific approaches to code environmental frequency information. Thus, it will be very interesting to investigate systemically how neurons in these pathways code peripheral stimulation of different frequencies.

Efforts have been made to clarify the central mechanism of frequency coding. Studies demonstrated that analgesia induced by different frequencies of peripheral electrical stimulation was organized in different brain areas. Specifically, the arcuate nucleus of the hypothalamus and the parabrachial nucleus of the pons play crucial roles in low- and high-frequency peripheral electrical stimulation-induced analgesia, respectively (Wang et al., 1990a,b, 1991). Histological study of c-*fos* expression suggested that overlapped but distinct neuronal networks were activated by these two frequencies (Guo et al., 1996). It has also been hypothesized that distinct low- and high-frequency processing modes exist in SI, and more generally the vibrissa sensory system (Moore, 2004).

However, no research has been conducted on the ensemble responses of the thalamocortical pathway neurons to peripheral electrical stimulation of a wide frequency range. How these neurons detect stimulation frequencies and 'control' the frequency-specific responses has yet to be determined. The present study was conducted to investigate the ensemble neuronal response of VP and SI, the somatosensory projection pathway, as well as medial dorsal thalamus (MD) and anterior cingulate cortex (ACC), the more subconscious sensory pathway, to peripheral electrical stimulation of 1 to 100 Hz in awake rats. The multichannel singe-unit recording technique was employed, which has been proved to be suitable for the study of ensemble neuronal activities (Fanselow et al., 2001; Ghazanfar et al., 2000; Katz et al., 2001; Nicolelis et al., 1993, 1995, 1997, 1998; Nicolelis and Chapin, 1994; Wang et al., 2003, 2004; Williams et al., 1999). Our working hypothesis is that the intrinsic electrical property of neural circuits might render them sensitive to stimulation of specific frequencies. Hence, the frequency-dependent neuronal responses should be at neural circuit, or cell assembly level. If this hypothesis is true, we should expect scattered frequency-specific responses across different brain areas.

Materials and methods

Subjects

The experiment was performed on eight male Sprague–Dawley rats weighing 300–350 g. The rats were provided by the Animal Service Center of Peking University Health Science Center. Animals were housed individually, with ad lib access to food and water, on a reverse light–dark schedule with the light phase started at 7:00 p.m. All experiments were carried out in accordance with the standards for use of laboratory animals established by the Institute of Laboratory Animal Resources, U.S. National Academy of Sciences, and with the Institutional Animal Care and Use Guideline of Peking University. All efforts have been made to minimize animal suffering and to reduce the number of animals used.

Implantation of recording electrodes

Rats were administered penicillin (16,000 U, i.m.) before surgery to prevent infection. Neural activity was recorded from the anterior cingulate cortex (ACC), primary somatosensory cortex (SI), medial dorsal thalamus (MD), and ventral posterior thalamus (VP). With each animal under ketamine anesthesia, four small craniotomies were made for microelectrode array implantation, as described by Nicolelis et al. (1997) and Wang et al. (2003). Coordinates for the craniotomies were according to the atlas of Paxinos and Watson as follows: (1) for SI, 1.0 mm posterior to bregma (−1.0 A), 2.0 mm lateral to midline (L), and 2.0 mm ventral to the skull surface (V); (2) for ACC, 3.2 A, 0.8 L, and 2.8 V; (3) for MD, −2.3 A, 0.8 L, and 5.6 V; (4) for VP, −3.0 A, 3.2 L, and 6.0 V. Four arrays of 8 Teflon-insulated stainless steel microwires were slowly lowered into the target areas. When the electrodes were in the correct locations, they were cemented to the skull with dental acrylic. Rats were allowed to recover for a week before recording sessions began.

Recording procedures

Neural electric signals were obtained from the stainless steel microwires and passed from the headset assemblies to a preamplifier via two lightweight cables and a commutator. The time resolution for data collection was 50 kHz. The signals were band-pass filtered between 0.5 and 5 kHz (6 dB cutoff) before being sent to a spike-sorting device. Spike activities were monitored on a computer. Waveforms were picked up by setting proper parameter pairs for amplitude and duration, and recorded into a database file with a PC-based software *Magnet* (Biographics, Inc. USA). The identity of clearly sorted single neurons was verified by graphical capture of waveforms. Data were then analyzed with commercially available PC-based programs *STRANGER* (Biographics, Inc. USA) and *Nex* (Plexon, Inc. USA). The animals' behaviors during the stimulation session were videotaped using a video camera (Vigour, VG-2012, China) recording 30 frames per second.

Stimulation protocol

During the recording session, rats were awake and slightly restricted in a hanging-up waistcoat with their

heads, limbs, and tails moving freely. Rats were trained to get familiar with the waistcoat for 3–4 times till they can stay quietly in it. Electrical stimuli were generated by a stimulator Pulsemaster A-300 and DC powered isolator A365 (World Precision Instrument, Inc. USA), applied to the glabrous skin of the hindpaws contralateral to the recorded sides. The parameters were: intensity 0.6 mA, pulse width 300 μs; and frequencies were increased stepwise from 1 to 100 Hz. Due to the 1-ms temporal resolution controlling the stimulation pulses delivery, only 53 frequencies (i.e., 1–34, 36–38, 40, 42, 43, 45, 48, 50, 53, 56, 59, 63, 67, 71, 77, 83, 91, and 100 Hz) were actually generated. Each frequency of stimulation lasted 1 min, during which a 5-s on/5-s off alternative schedule was employed. Each of the 1-min stimulation periods was followed by a 1-min resting period. The neural activities in resting period were recorded as control.

Data analysis

Quantification of neural signals

Peri-stimulation time histograms (PSTHs) of all recorded units and for all 53 frequencies were calculated in *Nex*, with a time range of $[-0.5 \times 1/f$ to $0.5 \times 1/f]$ (where f is the stimulation frequency), and a bin size of 10, 5, 3, 2, 2, and 2 ms for 1–6 Hz, respectively, and 1 ms for other frequencies. The results were then exported to *MatLab* in a spreadsheet format. In all analysis, the first 2-ms data after each stimulation pulse were removed, so as to eliminate the electrical artifacts that could be observed in the 0–2 ms time bins on some channels. Within the stimulation cycle $1/f$ (in seconds) of each frequency f, the maximal and minimal values of each PSTH (M_{max} and M_{min}) were located and transferred into Z scores (Z_{max} and Z_{min}). The value $Z_{max} - Z_{min}$ was employed to quantify the relative response magnitude of this neuron to this particular frequency. These response magnitude ($Z_{max} - Z_{min}$) values for all neurons and all 53 frequencies were then arranged into a spreadsheet. A clustering analysis (K-means, SPSS) was performed to classify the frequency response patterns of these neurons.

Latency and phase of peak responses

The latency of peak responses was detected, and transferred into phases in the stimulation cycle. To determine whether a given peak response is valid, the distribution of Z_{max} or Z_{min} in a randomized *Gaussian* distribution of the same size was determined by a *Monte Carlo* simulation procedure proposed by Douglas Ward (http://afni.nimh.nih.gov/afni/AFNI_Help/AlphaSim.htm). The upper 5% limit of this distribution was taken as the significant threshold. Latencies of significant responses were transformed into phases in the cycle by dividing the latency with the length of the cycle: phase = latency / Cycle-length.

Partial directed coherence

To identify the amount and direction of information flow among ACC, SI, MD, and VP, the method partial directed coherence (PDC) was used. This technique is able to express the notion of Granger causality (Granger, 1969) in the frequency domain and has been described in detail elsewhere (Sameshima and Baccalá, 1999; Baccalá and Sameshima, 2001; Fanselow et al., 2001). Briefly, PDC allows the uncovering of the direct influence exerted among simultaneously measured multichannel recorded data by highlighting neuronal groups that possibly drive other neuronal groups. Our first step was to find the first principal component (PC1) of all the neural responses within a given area and use them to calculate PDC (in 1–100 Hz range) around the onset of the 5-s stimulation epoch for each stimulation frequency. The mean PDC values were then normalized to the prestimulus baseline level, 3-s before the onset of the 5-s stimulation epoch as Z scores, i.e.,

$$Z_{\mathrm{PDC}} = \left(\mathrm{PDC}_{\mathrm{episode}} - M_{\mathrm{prestimulus}}\right)/S_{\mathrm{prestimulus}},$$

where Z_{PDC} is the normalized value of PDC (Z scores), $PDC_{episode}$ is the value from PDC analysis, $M_{prestimulus}$ and $S_{prestimulus}$ are mean and standard deviation of the baseline PDC, respectively. To show the patterns of information flow under stimulation for each frequency, the normalized PDC was then summarized either along the whole frequency range (i.e., peri-stimulus total PDC, see Fig. 5D) or across the 5-s stimulation epoch and rest epoch (i.e., PDC during stimulation and during rest, see Fig. 5E).

Histology study

Following the conclusion of recording, subjects were overdosed with ketamine. Recording sites were marked by electrophoretically deposited iron (10–20 μA DC current, 10–20 s duration, anode at the electrode) at the tips of selected wires. Animals were then perfused with 4% paraformaldehyde and their brains were extracted. The brains were post-fixed in a solution of 5% potassium ferricyanide/4% paraformaldehyde for several days. Coronal sections (40 μm) were cut through the SI, ACC, and thalamus. The iron deposits were easily identified as blue dots.

Fig. 1. Example of the peri-stimulus time histograms (PSTH) of (A) a typical excitatory neural responses of a SI neuron after 5-Hz stimulation, and (B) a MD neuron with an inhibitory response after 30-Hz stimulation. Vertical solid lines indicate the time of stimulus presentation (0 ms). The waveform of each neuron is shown on the upper right corner of the panel. (C) A SI neuron shows frequency-specific response to 5–9 Hz stimulation. (D) Response of neurons from one animal to 6 Hz stimulation, with different latencies.

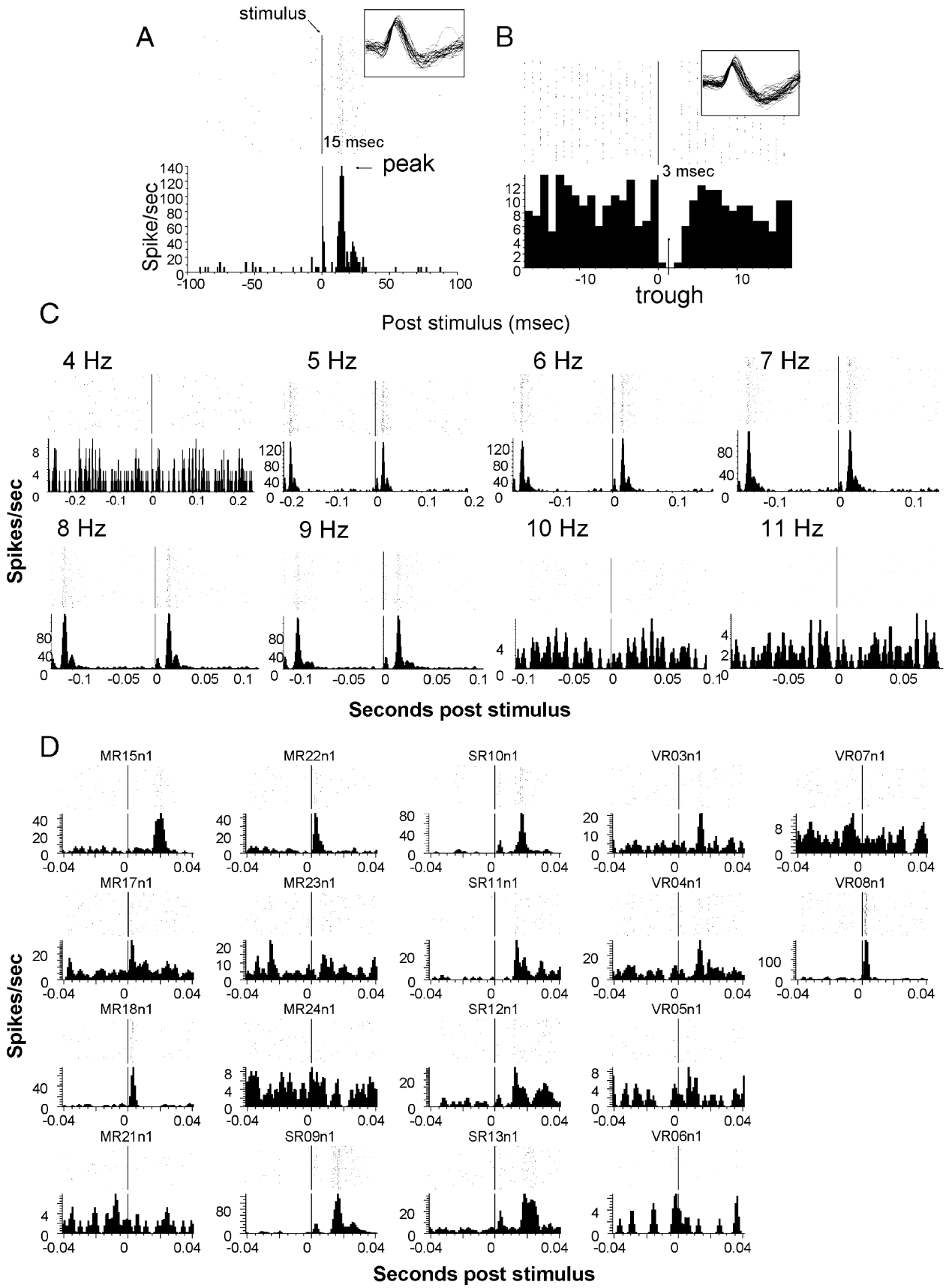
A
stimulus
15 msec
peak
Spike/sec
B
3 msec
trough
Post stimulus (msec)
C
4 Hz
5 Hz
6 Hz
7 Hz
8 Hz
9 Hz
10 Hz
11 Hz
Spikes/sec
Seconds post stimulus
D
MR15n1
MR22n1
SR10n1
VR03n1
VR07n1
MR17n1
MR23n1
SR11n1
VR04n1
VR08n1
MR18n1
MR24n1
SR12n1
VR05n1
MR21n1
SR09n1
SR13n1
VR06n1
Spikes/sec
Seconds post stimulus

Results

Behavioral response to electrical stimulation

All our rats adapted well to our restriction method. They stayed quietly during the experiment. Slight jiggling of the hindlimb muscle could be observed when stimuli were delivered. They caused no extra voluntary movement.

Response of single neurons to electrical stimulation

A total of 183 neurons (39 from ACC, 51 from MD, 51 from SI, and 42 from VP) were recorded from our subjects. Electrical stimulation from 1 to 100 Hz induced significant periodical variation of neural firing rates in each recording area. These responses were predominantly excitatory, although inhibitory ones were occasionally encountered. Typical excitatory and inhibitory responses are illustrated in Figs. 1A and B. Neuronal responses appeared to be frequency-specific, because each neuron usually responded to only a fraction of the stimulation frequencies (for example, see Fig. 1C).

The proportion of neurons exhibiting excitatory or inhibitory responses for each stimulation frequency is shown in Fig. 2. As depicted in Fig. 2A, less than 5% of total neurons were evoked by stimulations of 1–5 Hz. However, around 12–18% responded to stimulations of 5–10 Hz. This percentage gradually decreased until 70 Hz;

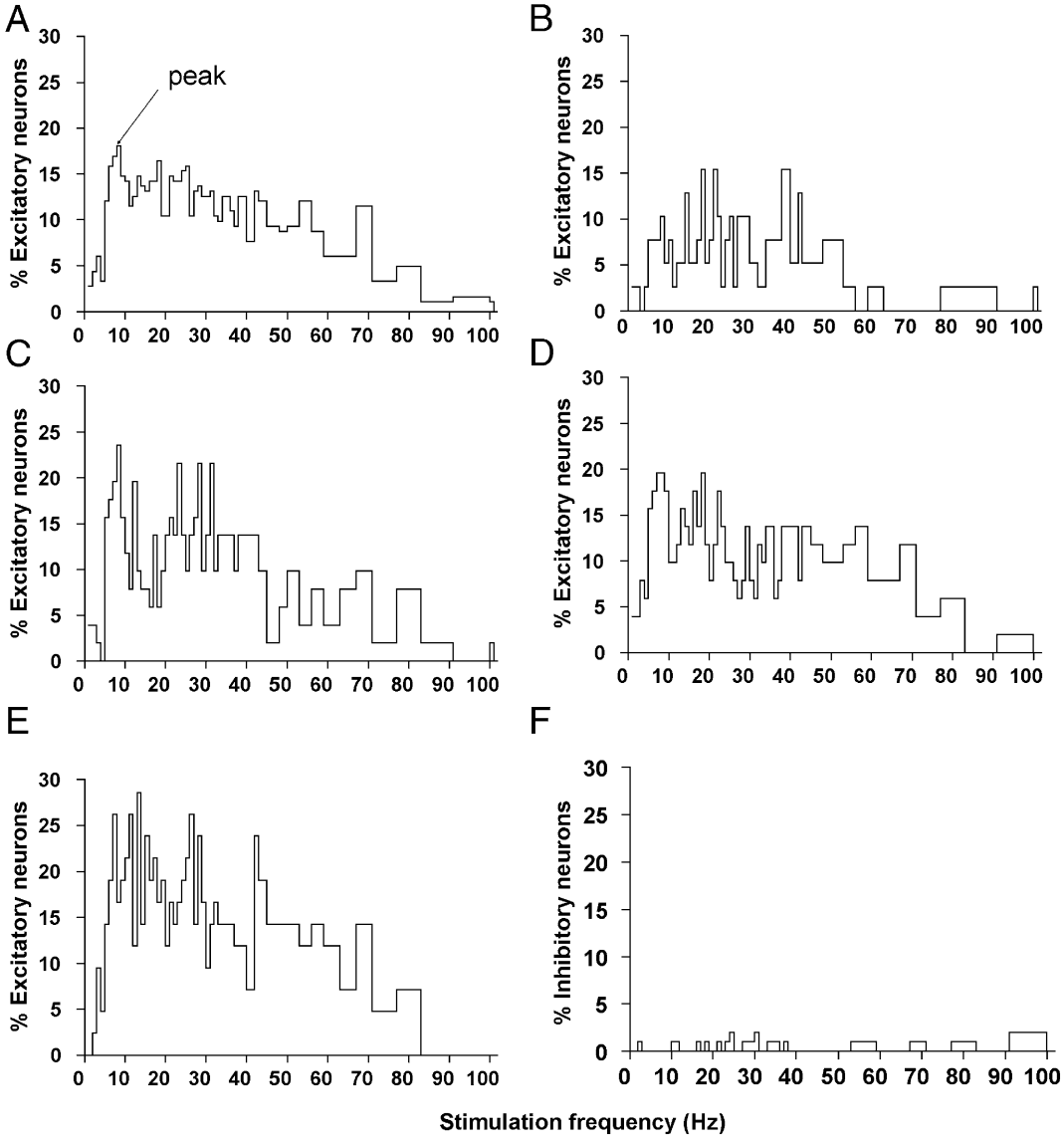

Fig. 2. Percentage of total neurons exhibiting excitatory or inhibitory responses to 1–100 Hz peripheral electrical stimulations. For excitatory response of all the four recording areas (A), the amount increased sharply to 12% at 5 Hz, and reached the peak to 18% at 8 Hz, then fluctuated and gradually decreased. After 70 Hz, responding neurons were lower than 5%. Percentage of excitatory neurons in (B) ACC, (C) SI, (D) MD, and (E) VP was also displayed. ACC processed the least responding neurons, lower than 15%; while VP owned the most, about 30%. And neurons in ACC, different from other areas, had little responses after 50 Hz. The responding pattern in SI and MD was similar to the overall excitatory pattern (A). On the contrary, inhibitory response is rare and scattered (F).

after that, it was again less than 5%. The percentage in ACC was lower than 15%. Moreover, less than 5% neurons had excitatory activities after 50 Hz (Fig. 2B). The responses in SI (Fig. 2C) and MD (Fig. 2D) were quite similar to the overall pattern of excitatory response. The percentage in VP was the largest, which reached 30% around 10 Hz. And the responses did not disappear until 80 Hz (Fig. 2E). Fig. 2F demonstrates the percentage of neurons exhibiting inhibitory responses. Only 1–2% neurons showed inhibitory responses to discrete frequencies.

To verify whether our consecutive stimulation mode may cause accommodation or habituation of the neurons, we delivered a brief 1-min 100 Hz peripheral electric stimulation to another group of eight rats, with the same stimulation parameters, and recorded neuronal responses from the same four brain areas. The result is shown in Table 1. Similar as with consecutive mode, single 100-Hz stimulation only activated a small portion of neurons from most of the recording areas. No significant difference was detected between two stimulation modes, except for the response of SI, which showed only a marginally significant difference (Chi-square test, $P = 0.0492$). We also tested the stability of resting period neuronal activities over the course of experiment by calculating the average firing rates of the 1-min resting periods after each stimulation period. As shown in Fig. 4F, no significant difference was observed among these resting periods (ANOVA, $P > 0.05$). From these results, we conclude that our stepwise experimental design has not generated significant accommodation/habituation. Thus, the decreased response proportion should be reflecting mainly the true frequency-specific response.

Coding of stimulation frequency with response magnitude

As explained in the Materials and methods section, $Z_{max} - Z_{min}$ in the PSTH was employed as the indicator of response magnitude of a neuron to a given frequency. These response magnitudes changed with stimulation frequency in different patterns, which could be revealed by our cluster analysis. As shown in Fig. 3A, the majority of neurons [156 of 183, cluster 5 (C5) and 6 (C6)] had peak responses before 10 Hz, and kept positive until 50 Hz. Most neurons in these clusters were strongly evoked in 5–10 Hz. Eleven neurons [cluster 1 (C1) and 2 (C2), indicated with red and green arrows in Fig. 3A] had robust responses specifically to

Table 1
Comparison of neuronal responses to consecutive and single 100-Hz stimulation

Stimulation mode	Responsive/total number of neurons in each area			
	ACC	MD	SI	VP
Consecutive	1/39	0/51	1/51	0/42
Single	5/56	4/57	9/76	3/71
P value*	0.3954	0.1203	0.0492	0.2931

* *P* values are the result of a *Chi*-square test between two stimulation modes. ACC: anterior cingulate cortex; MD: medial dorsal thalamus; SI: primary somatosensory cortex; VP: ventral lateral thalamus.

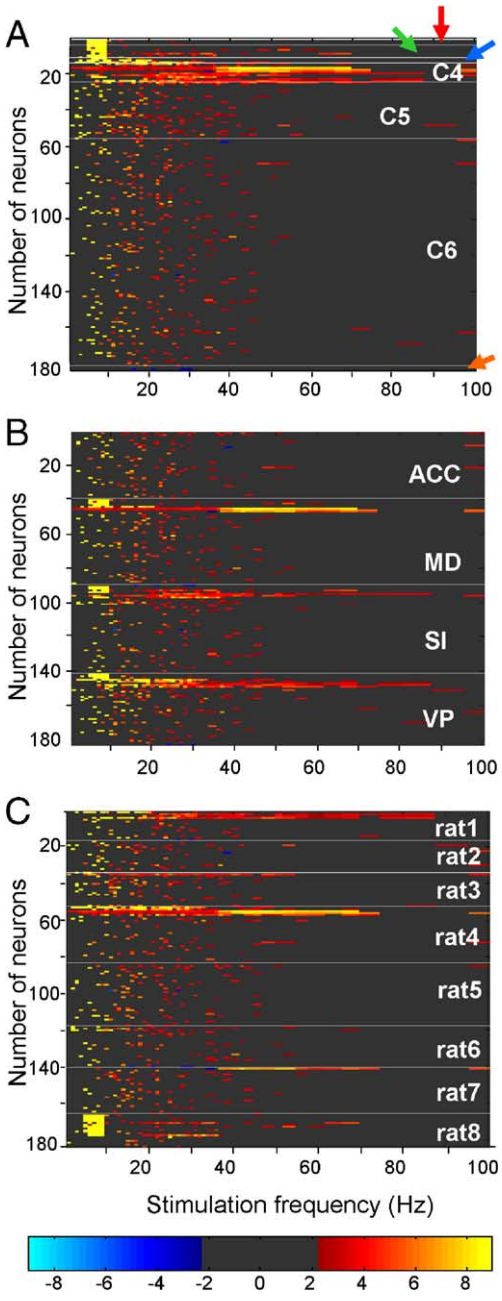

Fig. 3. The relative response magnitudes ($Z_{max} - Z_{min}$) of the PSTHs for each neuron and each stimulation-frequency were classified in (A) seven clusters. Clusters 1 (C1, indicated with red arrow) and 2 (C2, green arrow) were evoked remarkably in 5–9 Hz; cluster 3 (C3, blue arrow) had responses decreasing with the increase of frequency; cluster 4 (C4) exhibited positive response in most frequencies; cluster 5 (C5) and 6 (C6) neurons show peak responses before 10 Hz; while cluster 7 (C7, orange arrow) only had rare inhibitory responses. The *x*-axis represents the frequencies of peripheral electrical stimulations. The *y*-axis represents the number of neurons. Each line in the image represents the color-coded response of a neuron. (B) Neural response patterns of each recording brain region. The responding patterns in MD, SI, and VP were similar, while ACC did not have neurons showing continuous responses to successive frequencies. (C) The distribution of neural response patterns in 8 rats. The majority of response patterns could be found in all rats, except that C1 and C2 only happened in one rat.

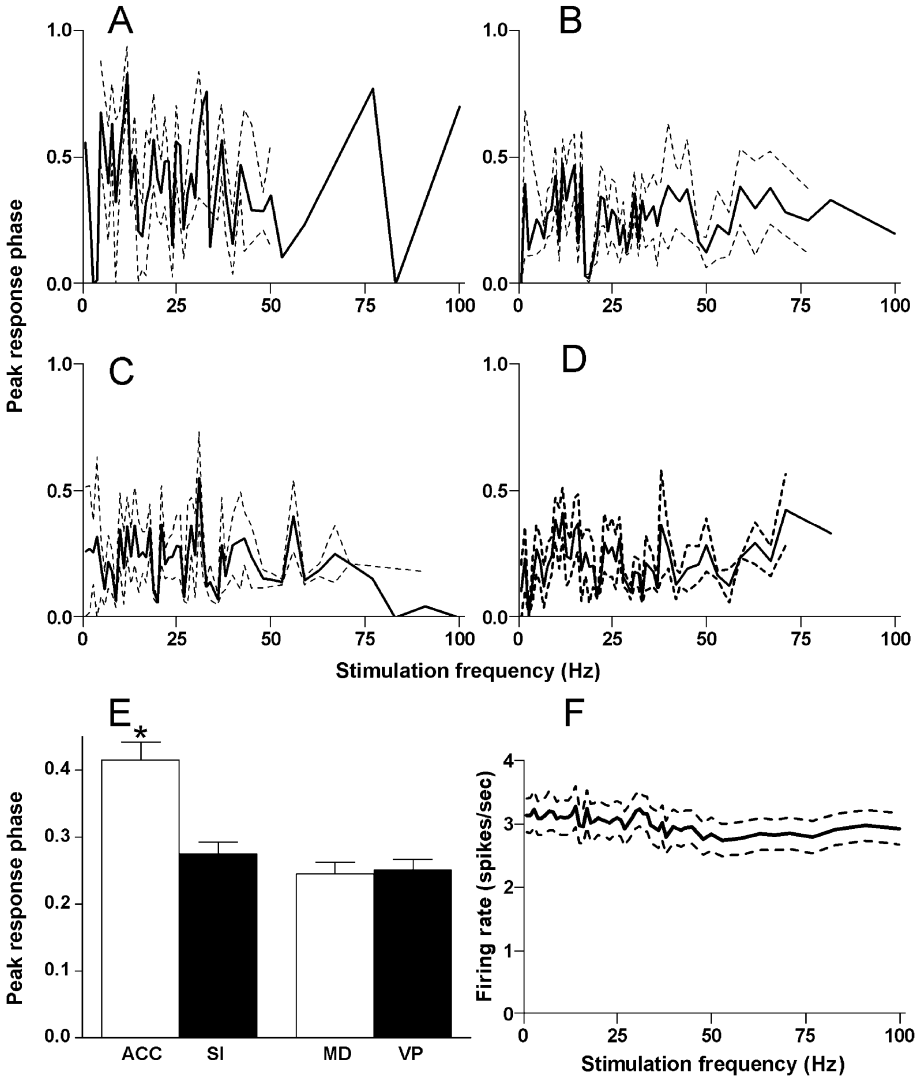

Fig. 4. The average peak responding phases of neurons in (A) ACC, (B) SI, (C) MD, and (D) VP. Phases in four areas vary with the increase of frequencies. However, ACC neurons respond significantly later in the cycle than the other three areas. Latencies in panels A, B, C, and D were summarized in a bar chart (E). It could be seen clearly that ACC neurons responded to peripheral stimuli in a significantly later phase of the cycle ($P < 0.05$). The average phase in ACC was above 0.4, while it was less than 0.3 in other three areas. (F) Mean firing rate during the 1-min resting periods after each stimulation period. No significant change is found among these data, showing a stable resting-period neural activity.

5–9 Hz (see also Fig. 1C for example). Three neurons [cluster 3 (C3), blue arrow in Fig. 3A] had responses decreasing sharply with the increase of frequency before 40 Hz; and 10 neurons in cluster 4 (C4) had stable and positive responses in most frequencies. Three neurons in cluster 7 (C7) had only negative responses in less than 10 frequencies. These patterns happened in all recording areas, except that ACC neurons failed to show any continuous responses to successive frequencies (C1–C4, see Fig. 3B). The majority of the response patterns could be seen in all rats, except for C1 and C2 only appearing in one rat (see Fig. 3C).

Coding of stimulation frequency with response phase

Neurons from the same animal may respond to the same stimulation frequency with different peak response latencies or phases (see Fig. 1D for an example). The frequency–response phase relationships are shown in Figs. 4A–D. The

Fig. 5. An example illustrating the process of partial directed coherence analysis. (A) PSTH of all SI (left) and VP (right) neurons at 6 Hz stimulation. Time = 0 on the transverse axis corresponds to the onset of the 5-s stimulation epoch. (B) PSTH of PC1 from SI (left) and VP (right). Each stimulus pulse evoked a clear increase of activity in SI. (C) PDC from SI to VP (left) and from VP to SI (right) was calculated from PC1. Stimulation evoked a decrease of PDC from SI to VP around 40 Hz, but increases of PDC from VP to SI in 1–30 Hz and 80–100 Hz ranges. (D) For each stimulation frequency, PDC was averaged along the whole range of coherence frequency to show the change of coherence with time. (E) PDC was averaged across the 5-s stimulation epoch for each stimulus frequency. (F) Summary of the results of the lines portrayed in Figs. 4D and E for all stimulation frequencies. The lines of 6 Hz are pointed out by black arrows. Since the frequencies after 34 Hz are discrete numbers, the corresponding lines are widened to fill the blank. For example, the line of 83 Hz is 7 times as wide as the line of 1 Hz.

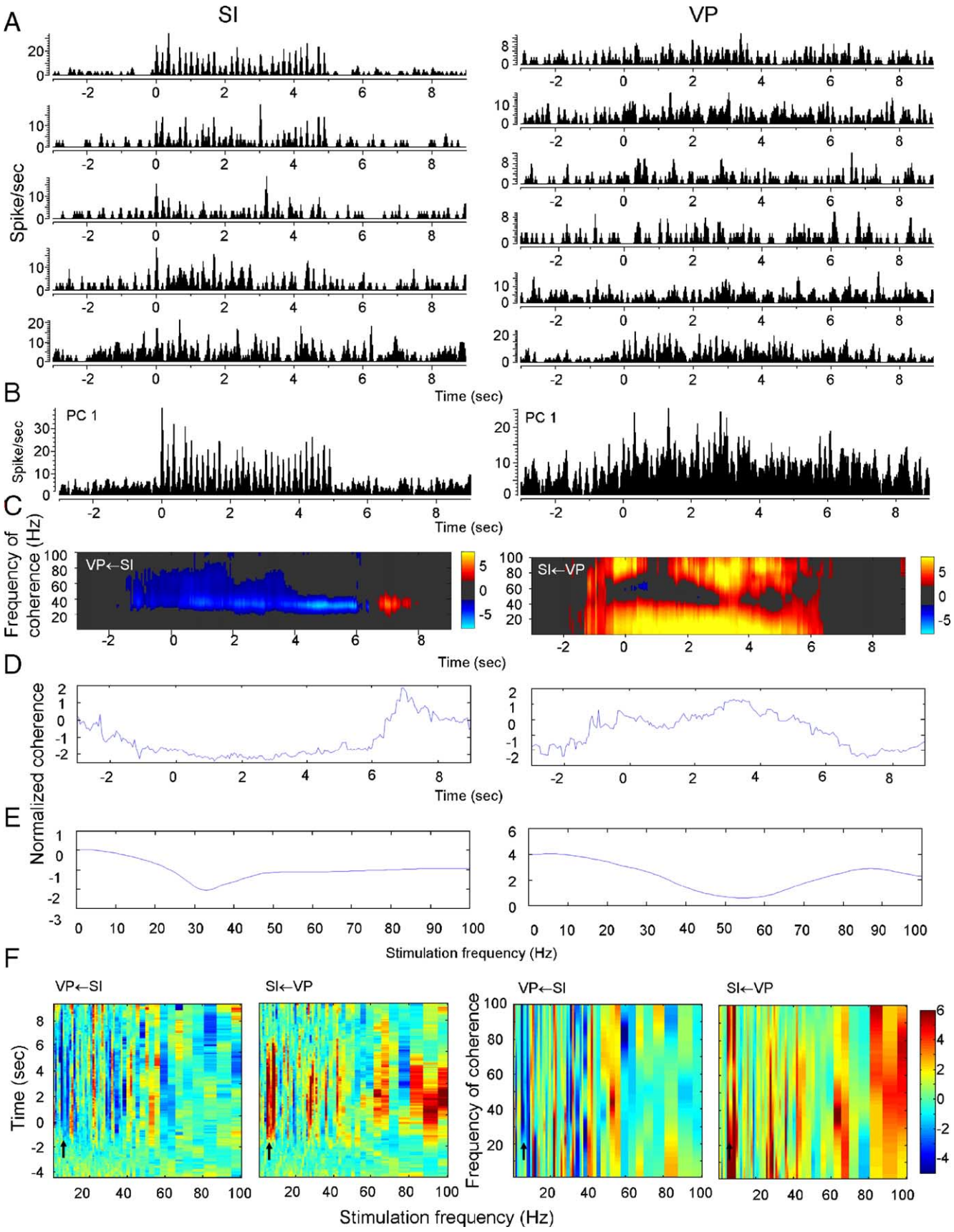
A
SI
VP
Spike/sec
Time (sec)
B
PC 1
PC 1
Spike/sec
Time (sec)
C
Frequency of coherence (Hz)
VP←SI
SI←VP
Time (sec)
D
Normalized coherence
Time (sec)
E
Stimulation frequency (Hz)
F
VP←SI
SI←VP
VP←SI
SI←VP
Time (sec)
Frequency of coherence
Stimulation frequency (Hz)

average response phases in a stimulation cycle of all recording areas vary with stimulation frequency, ranging from 0.1 to 0.8 cycle. Generally, the phases of cortical neurons were later than those of thalamic neurons. The phases in ACC were particularly late (Fig. 4A), and VP neurons did not show any phase later than 0.4 cycle (Fig. 4D). The averaged phases across all frequencies were summarized in Fig. 4E. It could be seen clearly that ACC neurons responded to peripheral stimuli in a significantly later phase of the cycle ($P < 0.05$). The average phase in ACC was around 0.42 cycle, while it was 0.24–0.27 cycle in other three areas.

Change of information flow pattern with stimulation frequency

We used PDC analysis to determine the change of information flow among the four recording areas during the stimulating as well as the resting epoch of each frequency. An example of the process of PDC analysis is illustrated in Fig. 5. In this example, the 5-s stimulation epoch induced a clear increase of firing activities in SI and VP neurons (Fig. 5A), which was more clearly displayed with their principle components (Fig. 5B). Stimulation of 6 Hz evoked a significant decrease of PDC from SI to VP around 40 Hz, but increased PDC from VP to SI in 1–30 Hz and again in 80–100 Hz ranges (Figs. 5C and E). This effect happened throughout the whole stimulation epoch (Fig. 5D). This coding pattern changed with frequency of stimulation, in terms of the direction, relative amount, temporal scale of PDC (Fig. 5F, left two panels), and peak frequency of PDC (Fig. 5F, right two panels). Since the stimulation frequencies (x-axis in Fig. 5F) after 34 Hz are discrete numbers, we widened the lines accordingly to fill the blank.

The average changes of PDC between the 4 recording areas from 8 rats are shown in Fig. 6. During the 5-s stimulation epoch, information flow increased or decreased in some frequency ranges, and the responding patterns varied among brain areas. For example, information flow from ACC to MD increased greatly in 59 Hz throughout the stimulation epoch (Fig. 6A, the panel on the second row of the first column). However, after averaging, the scale of response dropped considerably due to the canceling-out of the positive and negative changes of PDC (Fig. 6A). Thus, we re-calculated the average of the absolute value of PDC changes. A complex frequency coding pattern could be seen in terms of the amount and temporal scale of PDC changes (Fig. 6B). The response patterns of each brain region differed to a large extent. It could be noticed that the information flow changed dramatically in some specific frequency ranges. Again, the information flow from ACC to MD changed greatly in 59 Hz throughout the stimulation epoch (Fig. 6B, indicated with the black arrow).

The average absolute value of PDC changes in frequency domain is depicted in Fig. 7. A complex coding pattern of the stimulation frequency with frequency domain in PDC can be seen clearly, i.e., specific stimulating frequencies evoked strong responses in certain frequency ranges. For example, the 59 Hz stimulation induced increase of PDC in the range of 1–40 Hz (Fig. 7A, the panel in the second row of the first column). In contrast, variations of PDC in the resting phase were weaker and rarely seen (Fig. 7B).

Although it has been reported that neuronal oscillation can track peripheral stimulation frequency (Ahissar and Vaadia, 1990), this was not found in our averaging result. However, we did find a few individual neurons that showed frequency-locked responses, even during the 5-s resting epoch. This was shown as a frequency-locked coding-pattern in un-normalized PDC during the resting epoch from MD to VP in one rat (Fig. 7C).

Histology

The location of microwires as revealed by the iron deposits at the tips of selected microwires was depicted in Fig. 8, in which the black dots labeled the recording sites. As indicated in the figure, in the cingulate cortex, most of the iron deposits were found in the anterior areas; in the somatosensory cortex, most of the recording tips were in the hindlimb region; in MD, tips were mainly found in the mediodorsal part; in VP, the tips were primarily located in ventroposterior part.

Discussion

This study would be the first report characterizing the simultaneously recorded single-neuron response pattern of ACC, SI, MD, and VP to 1–100 Hz peripheral electrical stimulation. In agreement with earlier reports (Ahissar et al., 1997; Han, 2003; Moore, 2004), we found that cortical and thalamic neurons exhibited frequency-specific responses at both single-neuron and ensemble level. Neurons had various frequency coding patterns, as reflected by the percentage of responding neurons in each brain area, the relative scale of response, and the alteration of the amount and direction of information flow. Most neurons did not track the peripheral stimulation frequencies, but responded in their own patterns. This is consistent with the signature of cell assembly organization proposed by Harris (2005). It is also consistent with our hypothesis that the response of these neuronal circuits to different frequencies may largely depend on their intrinsic electrical properties. We suppose that peripheral stimulation may first evoke a synchronization propagating among neural assemblies in thalamus and cortex. Oscillation of neural circuits may then be evoked if their basic dynamic features meet the property of stimuli. These circuits, in turn, may send signals through their projection to other brain areas, and thus influence the function of a broader range of the nervous system.

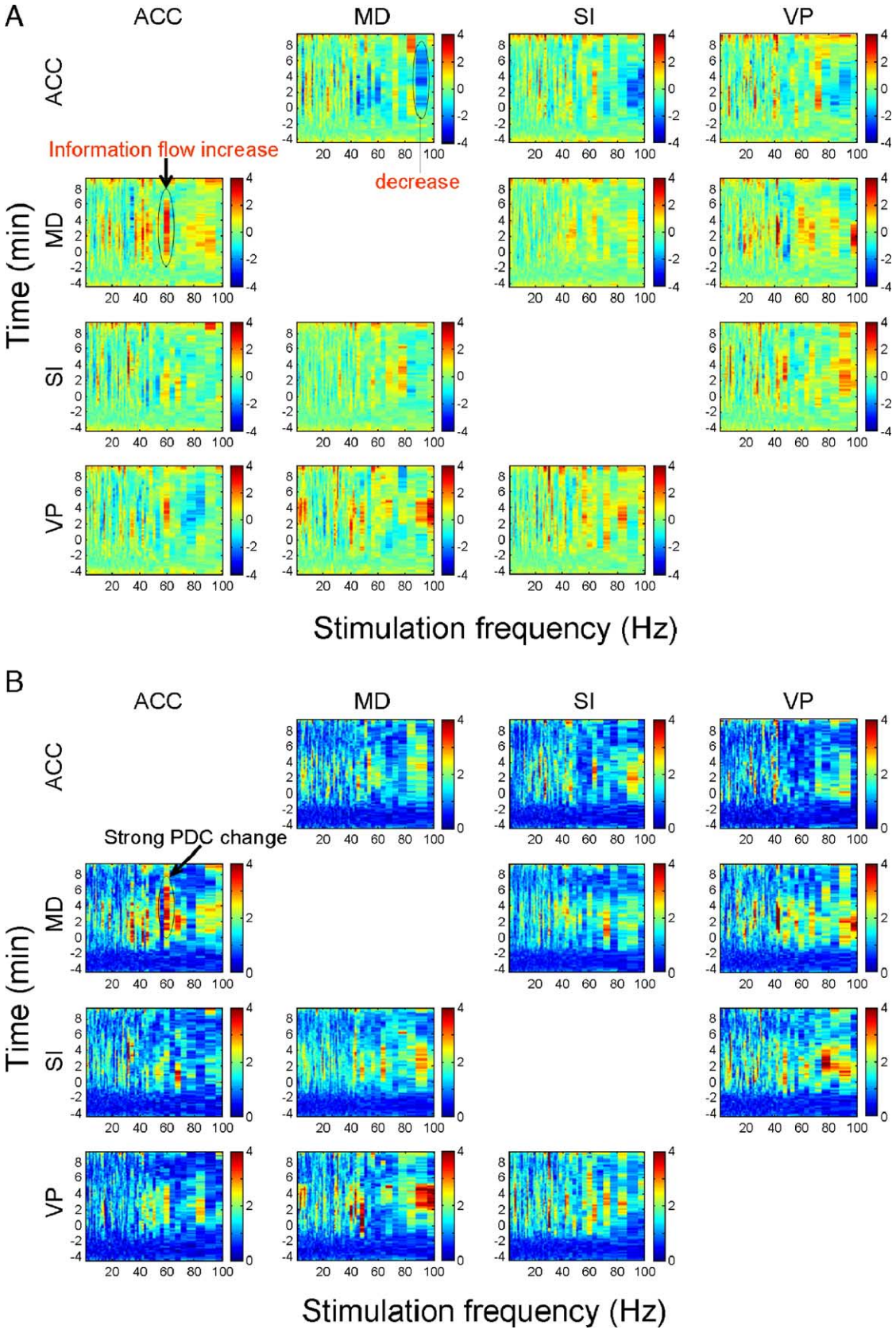

Fig. 6. The average changes of PDC among the 4 brain regions from 8 rats. (A) The information flow between every two areas was increased (shown in yellow and red) or decreased (shown in cyan and blue) in specific frequency ranges. (B) Absolute value of PDC changes. PDC changed dramatically in 5-s stimulation epoch compared with the 5-s resting epoch. Specific change of PDC could be observed in certain frequency ranges. Arrow indicates an example of strong PDC change from ACC to MD during 59 Hz stimulation.

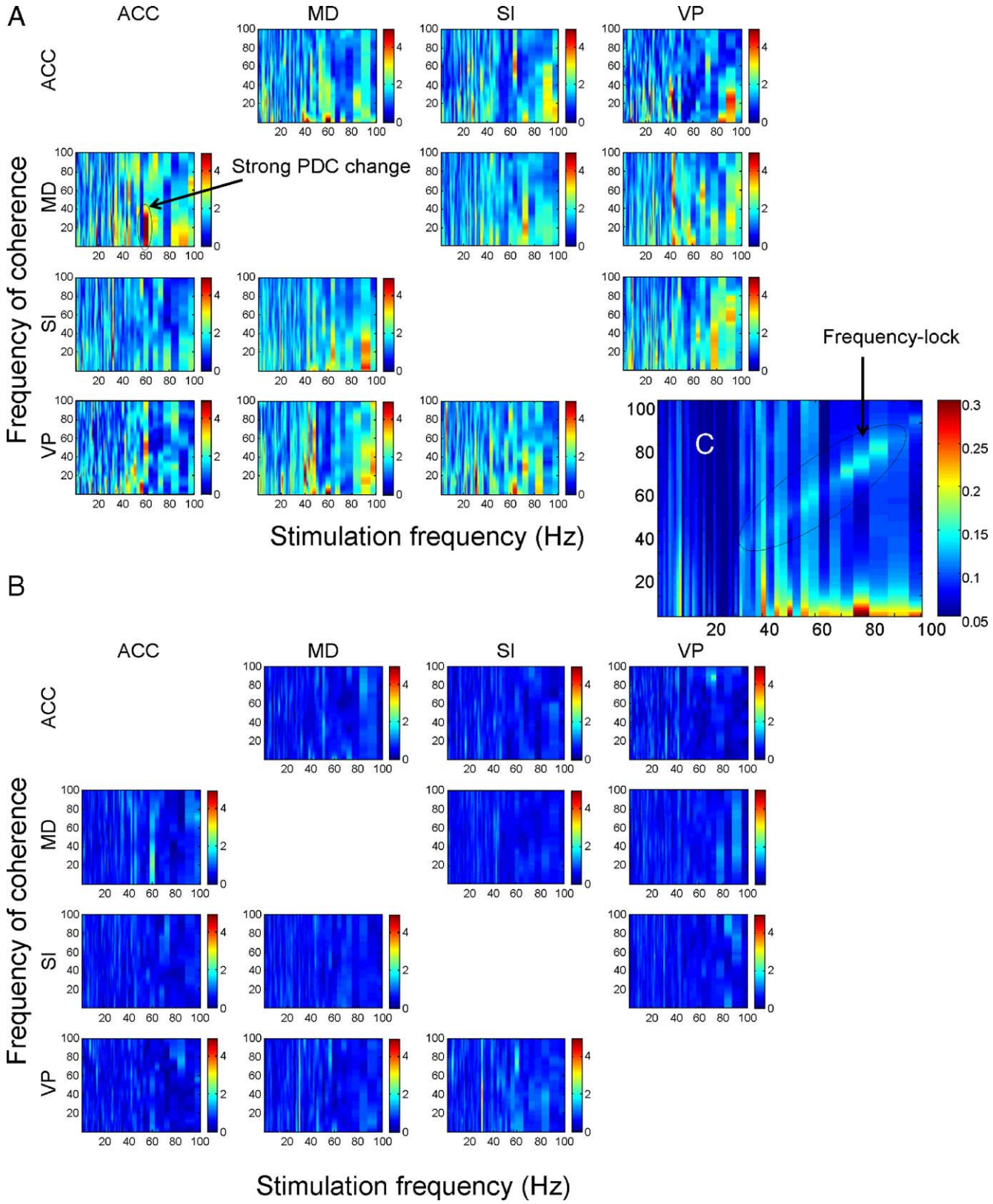

Fig. 7. The average absolute change of PDC in frequency domain in (A) stimulation epoch and (B) resting epoch. The variation of PDC displayed complex patterns in certain frequency range during stimulus epochs. The stimulus and resting epochs were in clear contrast. Arrow indicates a strong PDC change from ACC to MD around 20 Hz. (C) The frequency-locked coding pattern in one rat, as depicted with un-normalized PDC from MD to VP in the resting epoch.

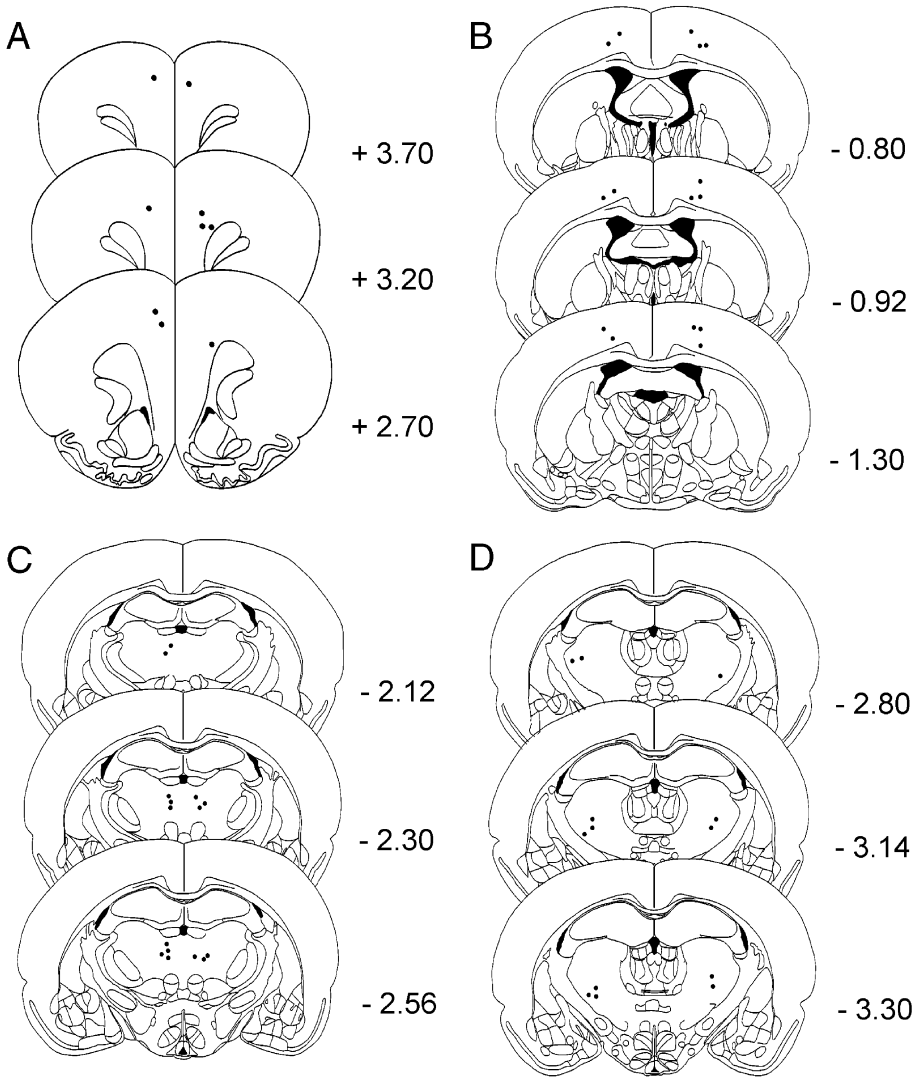

Fig. 8. A schematic drawing indicates the location of recording sites in ACC (A), SI (B), MD (C), and VP (D). The black dots labeled the position of iron deposits at the tips of selected microwires. Numbers on the right side of each panel indicate the number of millimeters a slice is rostral (+) or caudal (−) to the bregma.

Large-scale responses in CNS enabled by synchronization

A possible mechanism to evoke large-scale frequency-dependent responses in CNS is that synchronization will automatically happen with stimulation. This synchrony, which has been demonstrated to play a crucial role in signal propagation, could develop under a wide range of stimulus conditions and network configurations (Reyes, 2003). It occurs due to correlated activation at stimulus onset. Synchrony facilitated the spread of frequency-specific responses of neural assemblies, which can be defined as distributed local networks of neurons transiently linked by reciprocal dynamic connections (Varela et al., 2001). Therefore, neurons excited directly by peripheral stimuli can influence other assemblies and produce greater effects. The spread of synchrony can be controlled by lateral inhibition (Marchetti and Reyes, 2004), thus it will not cause epileptic global synchronization across the whole brain.

Role of intrinsic property of neural circuits

According to our results, peripheral stimulation could drive cortical and thalamic neural activities in different frequency ranges, but most neurons did not track the frequency of peripheral stimulation, instead they responded in their own patterns. We suppose that the frequency selectivity of neurons may be related to their intrinsic dynamic properties. Dynamic clamp studies proved that network dynamics arise from the interaction of intrinsic neuronal properties and synaptic strengths, hence producing a specific output pattern (Destexhe and Marder, 2004). Thus, a neural circuit does not actually select which peripheral frequency it is going to respond to. It is the peripheral stimulation itself that can either enhance or reduce the neural activity, depending on the electrical features of the neural circuits, or cell assemblies.

A wide range of parameters may converge to the same frequency-dependent property. It has been estimated that

similar changes in network function can arise from very different changes in parameters (Goldman et al., 2001; Prinz et al., 2004). Work on the pyloric rhythm in lobsters indicates that individual identified neurons may show considerable variability in their underlying conductance densities while maintaining the same functional feature, as long as appropriately correlated and compensating value of conductance exists. Synapse strength and cell distributions of hundreds of model pyloric networks could generate virtually the same output (Prinz et al., 2003, 2004). The intrinsic properties of the same neuron in different animals might be more variable than the network behavior in different animals; the strength of a given synapse in different animals might be more variable than network behavior in different animals (Prinz et al., 2003, 2004). Thus, the frequency-dependent responding patterns revealed in our results may derive from many different mechanisms, i.e., different combinations of cell membrane properties and synaptic strengths of the involved neural circuits. This may be part of the reason why stimulate-evoked responses were not specifically confined to certain areas, but distributed widely in the brain.

The largest percentage of neurons, about 15–20%, in our results responded to stimuli at 5–10 Hz. Also, the strongest response of 126/183 neurons emerged at this frequency range. In particular, 11 neurons had particularly strong responses at 5–9 Hz. Interestingly, Garabedian et al. (2003) who stimulated vibrissae at frequencies from 1 to 40 Hz also observed that both rate and temporal patterns of neural activity, measured as total spike rate or vector strength, show peak signal values at 5–10 Hz. It has been reported that a quarter of neurons being studied in rats exhibited clear spontaneous oscillations, many of them around 10 Hz (Ahissar et al., 1997). These spontaneous oscillations of neurons, which are one of their intrinsic properties, might enhance their responses to peripheral stimuli in this specific frequency range. Generally, independent neural oscillators with an intrinsic frequency that matches the rhythm of certain environmental events might participate in decoding this frequency information.

Functional implication

Neuronal circuits mobilized by peripheral stimuli with the aforementioned mechanisms may continue to project to other brain areas, and drive or modulate the behavior of other neural circuits. These projections could even go all the way down to the spinal cord. In this way, peripheral electric stimulation could exert a profound influence on the whole brain. This may be the mechanism of many frequency-specific effects of peripheral stimulation. For example, studies have demonstrated that a wide range of brain areas, such as the arcuate nucleus of the hypothalamus (ARH), parabrachial nucleus (PBN), and periaqueductal gray (PAG), all participate in mediating analgesia when 2 Hz or 100 Hz conditioning peripheral electric stimulation is applied on certain body sites (Han and Wang, 1992). More generally, it has been proved that 2- and 100-Hz stimulation induced markedly different spatial patterns of c-*fos* expression in the rat brain, suggesting there are overlapped but distinct neuronal networks underlying electroacupuncture of these two frequencies (Guo et al., 1996). These two networks then sent descending modulation on spinal cord local circuit, and release different neuropeptides, i.e., enkephalin for 2 Hz and dynorphin for 100 Hz, respectively (Fei et al., 1986; Han, 2003; Han and Sun, 1990; Ulett et al., 1998). This view is further proved by the fact that electrolytic and kainite lesion in ARH and PBN led to significant attenuation of the low- and high frequency-peripheral stimulation-induced analgesia, respectively (Wang et al., 1990a,b, 1991).

Knowledge about the frequency-dependent effects of electric stimulation may have many implications. Firstly, it helps to optimize parameters of clinical electric stimulation therapy. TENS or electroacupuncture has been proved useful for analgesia and a few other purposes (NIH Consensus Conference, 1998), but the related mechanisms are still not fully understood. Knowledge of frequency-dependent effects may help to define a proper frequency range for a special purpose. Secondly, the neuroscience bases of many other stimulation-induced effects are poorly understood. Our finding that peripheral electric stimulation has abundant frequency-specific effects indicates that there could be many more effects not yet proved or described. This opens a wide possibility for future development of electric stimulation therapy. Finally, the current study opens a new way of understanding how the central nervous system codes environmental frequency information, which is an important aspect of sensory perception.

Taken together, our results provide the first evidence that the central neuronal ensembles have complicated coding patterns for frequencies of peripheral electrical stimulation. Multiple mechanisms, including feedforward propagation, side inhibition, circuit oscillation, and distant projection and release of modulators, may be involved in these coding processes. This study also starts a new approach on modulating central activity with specifically tuned peripheral stimulation, which will have extensive clinical application.

Methodological concern

Central nervous system is known to develop plasticity easily. For example, repeated stimulation of low and high frequency is known to induce LTD and LTP in many brain areas, respectively (for a recent review of long-term plasticity, see Malenka and Bear, 2004). Thus, to observe the effect of many frequencies in a short experimental session will inevitably confront the risk of certain types of plasticity, given an ascending, descending, or randomized frequency sequence. Since we fixed the stimuli intensity, higher frequency may mean more energy

delivered into the central nervous system. Thus, a descending sequence might have bigger risk of plasticity. A randomized sequence might also bring about unpredictable influence on the result, given our small number of subjects. To compare the effect of different frequencies on the same group of neurons, it will equally be improper to do the experiment in many separate sessions. Hence, our design of ascending sequence in one session may be a better choice so far. Since our additional test of a brief 100-Hz stimulation on a separate group of rats generated approximately similar result considering the portion of neurons activated, and the firing rates of neurons in the resting periods did not change with the stimulation, we could safely say that our results mainly reflect the effect of each stimulation frequency, and the effect of accommodation/habituation, if ever exist, should be relatively weak.

Higher frequency of the same intensity may mean more delivered stimulation energy. However, it is hard to find a proper protocol to adjust the intensity for different frequencies. An improperly adjusted intensity schedule may bring unpredictable influence to the result. Thus, we decide to adopt an equal-intensity protocol. The intensity of 0.6 mA with a pulse width of 300 μs is sufficient to induce slight muscle twisting and, at the beginning of stimulation, vocal response, indicating that it is clearly a super-threshold stimulus. Since the firing pattern is not significantly influenced in the resting period in our study, and the neuronal response is in a frequency-related clustering manner rather than simple increasing or decreasing (see Figs. 1C and 3), it does not look like a simple summation of stimulation. Taken together, the effect we observed could be interpreted primarily as specifically related to stimuli frequencies.

Acknowledgments

The authors wish to thank Dr. Albert C.H. Yu for language editing and many constructive suggestions. This work was funded by the National Natural Science Foundation of China (30170307, 30370461), a grant from the 211 project, and two high-tech project grant ([2001] No. 50 and 2003CB515407) of China to F.L., NIH grants EB002092 and AA10980 to D.J.W., and NS-43441 and TW06144 to J.-Y.C.

References

Ahissar, E., Vaadia, E., 1990. Oscillatory activity of single units in a somatosensory cortex of an awake monkey and their possible role in texture analysis. Proc. Natl. Acad. Sci. U. S. A. 87, 8935–8939.

Ahissar, E., Haidarliu, S., Zacksenhouse, M., 1997. Decoding temporally encoded sensory input by cortical oscillations and thalamic phase comparators. Proc. Natl. Acad. Sci. U. S. A. 94, 11633–11638.

Ahissar, E., Sosnik, R., Haidarliu, S., 2000. Transformation from temporal to rate coding in a somatosensory thalamocortical pathway. Nature 406, 302–306.

Baccalá, L.A., Sameshima, K., 2001. Partial directed coherence: a new concept in neural structure determination. Biol. Cybern. 84, 463–474.

Destexhe, A., Marder, E., 2004. Plasticity in single neuron and circuit computations. Nature 431, 789–795.

Fanselow, E.E., Nicolelis, M.A.L., 1999. Behavioral modulation of tactile responses in the rat somatosensory system. J. Neurosci. 19, 7603–7616.

Fanselow, E.E., Sameshima, K., Baccalá, L.A., Nicolelis, M.A.L., 2001. Thalamic bursting in rats during different awake behavioral states. Proc. Natl. Acad. Sci. U. S. A. 98, 15330–15335.

Fei, H., Xie, C., Han, J.S., 1986. Differential release of metenkephalin and dynorphin in spinal cord by electroacupuncture of different frequencies. Chin. Sci. Bull. 28, 312–319.

Gao, X., Xu, D., Cheng, M., Gao, S., 2003. A BCI-based environmental controller for the motion-disabled. IEEE Trans. Neural Syst. Rehabil. Eng. 11, 137–140.

Garabedian, C.E., Jones, S.R., Merzenich, M.M., Dale, A., Moore, C.I., 2003. Band-pass response properties of rat SI neurons. J. Neurophysiol. 90, 1379–1391.

Ghazanfar, A.A., Stambaugh, C.R., Nicolelis, M.A.L., 2000. Encoding of tactile stimulus location by somatosensory thalamocortical ensembles. J. Neurosci. 20, 3761–3775.

Goldman, M.S., Golowasch, J., Marder, E., Abbott, L.F., 2001. Global structure, robustness, and modulation of neuronal models. J. Neurosci. 21, 5229–5238.

Granger, C.W.J., 1969. Investigating causal relations by econometric models and cross-spectral methods. Econometrica 37, 424–438.

Guo, H.F., Tian, J.H., Wang, X.M., Fang, Y., Hou, Y.P., Han, J.S., 1996. Brain substrates activated by electroacupuncture of different frequencies: I. Comparative study on the expression of oncogene c-*fos* and genes coding for three opioid peptides. Mol. Brain Res. 43, 157–166.

Han, J.S., 2003. Acupuncture: neuropeptide release produced by electrical stimulation of different frequencies. Trends Neurosci. 26, 17–22.

Han, J.S., Sun, M.Z., 1990. Differential release of enkephalin and dynorphin by low and high frequency electroacupuncture in the central nervous system. Acupunct. Sci. Int. J. 1, 19–27.

Han, J.S., Wang, Q., 1992. Mobilization of specific neuropeptides by periapheral stimulation of identified frequencies. News Physiol. Sci. 7, 176–180.

Harris, K.D., 2005. Neural signatures of cell assembly organization. Nat. Rev. Neurosci. 6, 399–407.

Kalcher, J., Flotzinger, D., Neuper, C., Golly, S., Pfurtscheller, G., 1996. Graz brain-computer interface: II. Towards communication between humans and computers based on online classification of three different EEG patterns. Med. Biol. Eng. Comput. 34, 382–388.

Katz, D.B., Simon, S.A., Nicolelis, M.A.L., 2001. Dynamic and multimodal responses of gustatory cortical neurons in awake rats. J. Neurosci. 21, 4478–4489.

Lozano, A.M., 2001. Deep brain stimulation for Parkinson's disease. Parkinsonism Relat. Disord. 7, 199–203.

Malenka, R.C., Bear, M.F., 2004. LTP and LTD an embarrassment of riches. Neuron 44, 5–21.

Marchetti, C., Reyes, A.D., 2004. Using Lateral Inhibition to Control Signal Flow in Iteratively-Constructed Networks. Society for Neuroscience, Washington, DC (Program No. 509.3. Abstract Viewer/Itinerary Planner).

Moore, C.I., 2004. Frequency-dependent processing in the vibrissa sensory system. J. Neurophysiol. 91, 2390–2399.

Nicolelis, M.A., Chapin, J.K., 1994. Spatiotemporal structure of somatosensory responses of many-neuron ensembles in the rat ventral posterior medial nucleus of the thalamus. J. Neurosci. 14, 3511–3532.

Nicolelis, M.A., Lin, R.C., Woodward, D.J., Chapin, J.K., 1993. Dynamic and distributed properties of many-neuron ensembles in the ventral posterior medial thalamus of awake rats. Proc. Natl. Acad. Sci. U. S. A. 90, 2212–2216.

Nicolelis, M.A., Baccalá, L.A., Lin, R.C., Chapin, J.K., 1995. Sensorimotor encoding by synchronous neural ensemble activity at multiple levels of the somatosensory system. Science 268, 1353–1358.

Nicolelis, M.A., Ghazanfar, A.A., Faggin, B.M., Votaw, S., Oliveira, L.M., 1997. Reconstructing the engram: simultaneous, multisite, many single neuron recordings. Neuron 18, 529–537.

Nicolelis, M.A., Ghazanfar, A.A., Stambaugh, C.R., Oliveira, L.M., Laubach, M., Chapin, J.K., Nelson, R.J., Kaas, J.H., 1998. Simultaneous encoding of tactile information by three primate cortical areas. Nat. Neurosci. 1, 621–630.

NIH Consensus Conference, 1998. Acupuncture. J. Am. Med. Assoc. 280, 1518–1524.

Pfurtscheller, G., Flotzinger, D., Pregenzer, M., Wolpaw, J.R., McFarland, D., 1995. EEG-based brain computer interface (BCI). Search for optimal electrode positions and frequency components. Med. Prog. Technol. 21, 111–121.

Pfurtscheller, G., Neuper, C., Guger, C., Harkam, W., Ramoser, H., Schlogl, A., Obermaier, B., Pregenzer, M., 2000. Current trends in graz brain-computer interface (BCI) research. IEEE Trans. Rehabil. Eng. 8, 216–219.

Pregenzer, M., Pfurtscheller, G., 1999. Frequency component selection for an EEG-based brain to computer interface. IEEE Trans. Rehabil. Eng. 7, 413–419.

Prinz, A.A., Billimoria, C., Marder, E., 2003. An alternative to hand-tuning conductance-based models: construction and analysis of databases of model neurons. J. Neurophysiol. 90, 3998–4015.

Prinz, A.A., Billimoria, C., Marder, E., 2004. Similar network activity from disparate circuit parameters. Nat. Neurosci. 7, 1287–1288.

Reyes, A.D., 2003. Synchrony-dependent propagation of firing rate in iteratively constructed networks in vitro. Nat. Neurosci. 6, 593–599.

Sameshima, K., Baccalá, L.A., 1999. Using partial directed coherence to describe neuronal ensemble interactions. J. Neurosci. Methods 94, 93–103.

Tarsy, D., 2001. Deep brain stimulation and movement disorder. Epilepsy Behav. 2, S45–S54.

Ulett, G.A., Han, S.P., Han, J.S., 1998. Electroacupuncture: mechanisms and clinical application. Biol. Psychiatry 44, 129–138.

Varela, F., Lachaux, J.-P., Rodriguez, E., Martinerie, J., 2001. The brainweb: phase synchronization and large-scale integration. Nat. Rev. 2, 229–239.

Wang, Q., Mao, L.M., Han, J.S., 1990a. The arcuate nucleus of hypothalamus mediates low but not high frequency electroacupuncture analgesia in rats. Brain Res. 513, 60–66.

Wang, Q., Mao, L.M., Han, J.S., 1990b. The role of periaqueductal gray in mediation of analgesia produced by different frequency electroacupuncture stimulation in rats. Int. J. Neurosci. 53, 167–172.

Wang, Q., Mao, L.M., Han, J.S., 1991. The role of parabrachial nucleus in high frequency electroacupuncture analgesia in rats. Chin. J. Physiol. Sci. 7, 363–367.

Wang, J.-Y., Luo, F., Chang, J.-Y., Woodward, D.J., Han, J.S., 2003. Parallel pain processing in freely moving rats revealed by distributed neuron recording. Brain Res. 992, 263–271.

Wang, J.-Y., Zhang, H.-T., Han, J.S., Chang, J.-Y., Woodward, D.J., Luo, F., 2004. Differential modulation of nociceptive neural responses in medial and lateral pain pathways by peripheral electrical stimulation: a multichannel recording study. Brain Res. 1014, 197–208.

Williams, J.C., Rennaker, R.L., Kipke, D.R., 1999. Long-term neural recording characteristics of wire microelectrode arrays implanted in cerebral cortex. Brain Res. Protoc. 4, 303–313.